

Experiments with Generalized Midpoint and Trapezoidal Rules on two Nonsmooth ODE's

P. Boeck, B. Gompil, A. Griewank, R. Hasenfelder, N. Strogies

January 18, 2014

Abstract

In this paper, we focus on generalized mid-point and generalized trapezoidal rules to validate the algorithmic proposal from [3] concerning the integration of ordinary differential equations with Lipschitz continuous right hand sides. We report numerical experiments for test problems and validate the convergence results.

Keywords: Lipschitz Dynamics, Piecewise Linearization, Midpoint and Trapezoidal Rule.

1 Motivation

Many realistic computer models are nondifferentiable in that the functional relation between input and output variables is not smooth. We are particularly focusing on Lipschitz continuous models where the nondifferentiabilities have a special structure. We present a technique that handles such functions in the context of ordinary differential equations (ODE's).

The technique is based on algorithmic differentiation (AD) and generalizes this concept. For further information on the general theory of AD we refer to [4, 8]. In contrast to the standard approach we allow for the occurrence of the nonsmooth but Lipschitz continuous elemental function absolute value $\mathbf{abs}(\cdot)$ and consequently all functions that are representable by it (e.g. $\min(\cdot, \cdot)$ and $\max(\cdot, \cdot)$).

Consider the following Initial Value Problem for an autonomous Ordinary Differential Equation (ODE).

$$\dot{x}(t) = F(x(t)), \quad x(0) = x_0 \quad (1)$$

Here, $x \in \mathbb{R}^n$ and $F : \mathbb{R}^n \rightarrow \mathbb{R}^n$ is vector valued and assumed to be locally Lipschitz continuous. It is well known, that this system has a unique local solution up to some time $\bar{t} > 0$. For any time-step $h > 0$ the exact solution of (1) satisfies

$$x^{l+1} = x^l + \int_{lh}^{(l+1)h} F(x(\tilde{t})) d\tilde{t}, \quad \text{for } l = 0, 1, \dots \quad (2)$$

with $x^l = x(hl)$ and $x^0 = x_0$. Naturally, the integral can not be evaluated exactly if only because the solution path $x(\tilde{t})$ is not known. As in the classical implicit midpoint and trapezoidal rule we first replace $x(\tilde{t})$ by the secant line

$$\bar{x}(\tilde{t}) = x^{l+1} \cdot (\tilde{t}/h - l) - x^l \cdot (\tilde{t}/h - (l+1)) \text{ for } hl \leq \tilde{t} \leq h(l+1) \quad (3)$$

Second, we suitably approximate $F(\bar{x}(\tilde{t}))$ by a piecewise linear function. The classical implicit midpoint rule applies the constant approximation $F(\bar{x}(\tilde{t})) \approx F(\bar{x}(h(l+1/2)))$ and the classical trapezoidal rule uses $F(\bar{x}(\tilde{t})) \approx F(x^{l+1})((\tilde{t}-hl)/h) - F(x^l)((\tilde{t}-h(l+1))/h)$. The integration of these approximations yield locally a third order truncation error $O(h^3)$ if F is Lipschitz continuously differentiable. When F is only Lipschitz continuous the truncation error is generally only of order

$O(h^2)$. To reestablish a truncation error of order three we will approximate $F(\tilde{x}(\tilde{t}))$ by a piecewise linear function that reflects possible kinks in F . The remainder of this note is organized as follows. In Section 2 we briefly summarize the notation and properties of piecewise linear functions. In Section 3 we recall the approximation properties of these functions when used for the integration of Lipschitz continuous functions. In Section 4 we validate the theoretical results with an academical example and one taken from electrical engineering.

2 Piecewise Linear Model

Definition 2.1. A continuous function $F : \mathbb{R}^n \rightarrow \mathbb{R}^m$ is called **piecewise linear** if there exist a finite number of linear **selection functions** $F_i : \mathbb{R}^n \rightarrow \mathbb{R}^m$ such that for any given $x \in \mathbb{R}^n$ there exist at least one index i with $F(x) = F_i(x)$. Here 'linear' is used in the sense of affine, i.e. allows a constant term $F_i(0) \neq 0$

Let the index set $I = \{1, \dots, k\}$ of the selection functions be given. Due to [9, Proposition 2.2.2] we can find subsets $M_1, \dots, M_l \subset I$ such that a scalar valued piecewise linear function f can be represented as

$$f(x) = \max_{1 \leq i \leq l} \min_{j \in M_j} F_j(x)$$

which will be referred to as **max-min representation**. This concept naturally carries over to vector valued functions F where we can find such a decomposition for every component of the image.

Piecewise linear functions are globally Lipschitz continuous and differentiable almost everywhere in the classical sense. Moreover, they are differentiable in the sense of Bouligand and Clarke. For a further discussion of these properties we refer to [9].

Next we consider continuous, piecewise differentiable functions F that can be computed by a finite program called evaluation procedure. More specific, we will allow the evaluation procedure of $F : D \subseteq \mathbb{R}^n \rightarrow \mathbb{R}^m$ to contain, in addition to the usual smooth elementary functions, the absolute value $\mathbf{abs}(x) = |x|$. Consequently, we can also handle the maximum and minimum of two values via the representation

$$\max(u, v) = (u + v + |u - v|)/2, \quad \min(u, v) = (u + v - |u - v|)/2$$

We call the resulting functions *composite piecewise differentiable*. The evaluation procedure of $y = F(x)$ can be interpreted as a directed, acyclic graph from $x = (v_{1-n}, \dots, v_0)$ to $y = (v_{l-m+1}, \dots, v_l)$ where the intermediate values $v_i, i = 1, \dots, l$ are computed by binary operations $v_i = v_j \circ v_k$ with $\circ \in \{+, -, *\}$ and $v_j, v_k \prec v_i$ or unary functions $v_i = \phi_i(v_j)$ with $v_j \prec v_i$ and

$$\phi_i \in \Phi = \{\exp(\cdot), (\cdot)^{-1}, \sqrt{(\cdot)}, \dots, \mathbf{abs}(\cdot)\}.$$

Here Φ represents a library of smooth elementals (at least on certain domains) and the nonsmooth elementals already introduced. The relation \prec represents the data dependence in the graph of the evaluation procedure which must be acyclic. We now want to compute an incremental approximation $\Delta y = \Delta F(\hat{x}; \Delta x)$ to $F(\hat{x} + \Delta x) - F(\hat{x})$ at a given \hat{x} and for a variable increment Δx . Assuming, that all functions other than the absolute value are differentiable, we introduce the following propagation rules.

$$\begin{aligned} \Delta v_i &= \Delta v_j \pm \Delta v_k & \text{for } \hat{v}_i &= \hat{v}_j \pm \hat{v}_k \\ \Delta v_i &= \hat{v}_j * \Delta v_k + \Delta v_j * \hat{v}_k & \text{for } \hat{v}_i &= \hat{v}_j * \hat{v}_k \\ \Delta v_i &= \hat{c}_{ij} \Delta v_j \quad \text{with } \hat{c}_{ij} = \varphi'(\hat{v}_j) & \text{for } \hat{v}_i &= \varphi_i(\hat{v}_j) \neq \mathbf{abs}(\cdot) \\ \Delta v_i &= \mathbf{abs}(\hat{v}_j + \Delta v_j) - \mathbf{abs}(\hat{v}_j) & \text{for } \hat{v}_i &= \mathbf{abs}(\hat{v}_j) \end{aligned} \tag{4}$$

Whenever F is globally differentiable (i.e., there are no \mathbf{abs} calls in the evaluating procedure) we get $\Delta y = F'(\hat{x})\Delta x$ where $F'(\hat{x}) \in \mathbb{R}^{m \times n}$ is the Jacobi-matrix. Concerning this piecewise differentiation we obtain the following elementary results proving the existence of the object $\Delta F(\hat{x}; \Delta x)$ and the corresponding approximation order.

Proposition 2.1. [3] Suppose F is composite piecewise differentiable on some open neighborhood D of a closed, convex domain $\mathcal{K} \in \mathbb{R}^n$. Then there exist a constant γ such that for all $x, \hat{x} \in \mathcal{K}$ we have

$$\|F(x) - F(\hat{x}) - \Delta F(\hat{x}; x - \hat{x})\| \leq \gamma \|x - \hat{x}\|^2.$$

Moreover, for $\tilde{x}, \hat{x} \in \mathcal{K}$ and $\Delta x \in \mathbb{R}^n$ we find

$$\frac{\|\Delta F(\tilde{x}, \Delta x) - \Delta F(\hat{x}, \Delta x)\|}{1 + \|\Delta x\|} \leq \tilde{\gamma} \|\tilde{x} - \hat{x}\|.$$

Note, that the propagation rules (4) rely on the so called tangent approximation of F at a certain point x . However, there are applications of piecewise linearization (especially concerning ODE integration) where one wants to consider approximations of F based on secants. Given two points \tilde{x}, \hat{x} we compute $\hat{x} = (\tilde{x} + \hat{x})/2$ and $\hat{F} = (F(\tilde{x}) + F(\hat{x}))/2$. Now we consider the secant approximation of F .

$$F(x) \approx \hat{F} + \Delta F(\hat{x}, \tilde{x}; x - \hat{x}) \quad (5)$$

The essential features of the two piecewise linearizations are displayed in in Figure 1.

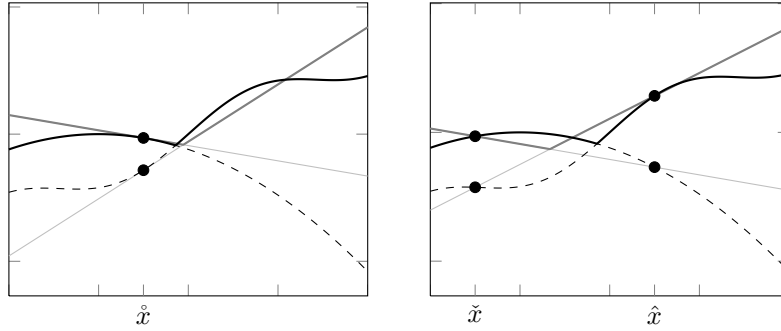


Figure 1: visualization of tangent and secant mode linearizations

In order to utilize AD for the algorithmic computation of the secant approximation in (5) we observe that in (4) the intermediate values can be seen as functions evaluated at the unique reference point \hat{x} , $\hat{v}_i = v_i(\hat{x})$. Now this reference point is the midpoint of \tilde{x} and the intermediate values are

$$\hat{v}_i = (\check{v}_i + \hat{v}_i)/2 \text{ with } \check{v}_i = v_i(\tilde{x}), \hat{v}_i = v_i(\hat{x}). \quad (6)$$

Replacing v_i with \hat{v}_i in (4) we observe, that the first and second line are the same for the secant linearization. The third line has to be changed slightly since the tangent slope \hat{c}_{ij} has to be replaced by the secant slope

$$\hat{c}_{ij} = \begin{cases} \phi'_i(\hat{v}_j) & \text{if } \check{v}_j = \hat{v}_j \\ \frac{\hat{v}_i - \check{v}_i}{\hat{v}_j - \check{v}_j} & \text{otherwise} \end{cases}$$

The last rule stays unchanged except that now $\hat{v}_i = (\check{v}_i + \hat{v}_i)/2 = (|\check{v}_j| + |\hat{v}_j|)/2$. Note that, if $\tilde{x} = \hat{x}$ we obtain $\Delta F(\hat{x}, \Delta x) = \Delta F(\tilde{x}, \hat{x}; \Delta x)$. A complete discussion on this implementation topic can be found in [3, Section 7]. Now the following approximation result holds.

Proposition 2.2. [3] Suppose F is composite piecewise differentiable on some open neighborhood D of a closed, convex domain $\mathcal{K} \in \mathbb{R}^n$. Then there exist a constant γ such that for all $\tilde{x}, \hat{x}, x \in \mathcal{K}$ we have

$$\|F(x) - (F(\tilde{x}) + F(\hat{x}))/2 - \Delta F(\hat{x}, \tilde{x}; x - \hat{x})\| \leq \gamma (\|x - \tilde{x}\| \|x - \hat{x}\|)$$

and

$$\frac{\|\Delta F(\tilde{x}, \hat{x}, \Delta x) - \Delta F(\tilde{z}, \hat{z}, \Delta x)\|}{1 + \|\Delta x\|} \leq \tilde{\gamma} (\|\tilde{x} - \tilde{z}\| + \|\hat{x} - \hat{z}\|)$$

In summary we can construct piecewise linear models of piecewise differentiable functions by the application of AD and immediately have the above approximation properties.

3 Generalized Integration Methods

The complete approximation theory can be found in [3] and [7]. As outlined in Section 1 we obtain a generalization of the classical implicit midpoint rule by a certain approximation to $F(x(\tilde{t}))$ in (2). Substituting $\tilde{t} = [(l+1/2) + \tau]h$ in (2) we obtain with $\tilde{x}(\tau) = \bar{x}((l+1/2 + \tau)h)$ for $-1/2 \leq \tau \leq 1/2$ the equation

$$x^{l+1} = x^l + \int_{-1/2}^{1/2} F(\tilde{x}(\tau))d\tau, \quad \text{for } l = 0, 1, \dots \quad (7)$$

Abbreviating $\hat{x} = x(h(l+1))$, $\check{x} = x(hl)$ and setting $\hat{x} = (\hat{x} + \check{x})/2$, we employ $F(\tilde{x}(\tau)) \approx F(\hat{x}) + \Delta F(\hat{x}; (\hat{x} - \check{x})\tau)$ and obtain the discretization

$$\hat{x} - \check{x} = h \int_{-1/2}^{1/2} F(\hat{x}) + \Delta F(\hat{x}; (\hat{x} - \check{x})\tau)d\tau \quad (8)$$

for any subinterval $[lh, (l+1)h]$. If F is continuously differentiable, the integral over the linearized part drops out and we obtain by $\hat{x} - \check{x} = hF(\hat{x})$ the classical implicit midpoint rule. Otherwise, we can utilize the piecewise linear nature of $\Delta F(\hat{x}; v)$ to evaluate the second part of the integral exactly for any given \check{x} and \hat{x} . The following result ensures, that the resulting method preserves the local truncation error of order three.

Proposition 3.1. [3] *There exist a step size bound $\bar{t} > 0$ such that for all $h \leq \bar{t}$ (8) attains a unique solution \hat{x} . Moreover we have the relation*

$$\hat{x} - x((l+1)h) = O(h^3)$$

where $x(t)$ solves $\dot{x}(t) = F(x(t))$ with $x(lh) = \check{x}$.

In order to construct a generalized trapezoidal rule we consider another approximation, $F(\tilde{x}(\tau)) \approx \mathring{F} + \Delta F(\hat{x}; \check{x}; (\hat{x} - \check{x})\tau)$ for $\mathring{F} = (F(\hat{x}) + F(\check{x}))/2$. Then we obtain

$$\hat{x} - \check{x} = h \int_{-1/2}^{1/2} \mathring{F} + \Delta F(\hat{x}; \check{x}; (\hat{x} - \check{x})\tau)d\tau \quad (9)$$

for the secant based piecewise linearization $\Delta F(\hat{x}; \check{x}; (\hat{x} - \check{x})\tau)$ of F . Again we observe, that this is a generalization of the classical method, since for smooth F we obtain the usual trapezoidal rule. Again we can prove, that the constructed method preserves a third order truncation error.

Proposition 3.2. [3, 7] *There exist a step size bound $\bar{t} > 0$ such that for all $h \leq \bar{t}$ (9) attains a unique solution \hat{x} . Moreover we have the relation*

$$\hat{x} - x((l+1)h) = O(h^3)$$

where $x(t)$ solves $\dot{x}(t) = F(x(t))$ with $x(lh) = \check{x}$.

In the remainder of this note, the term generalized midpoint rule refers to (8) while generalized trapezoidal rule denotes a method based on (9). Both are systems of piecewise smooth algebraic equations for which a special solver is under development. In other words the generalized midpoint and trapezoidal rules are like the original ones implicit. In the examples discussed in Section 4 everything can be reduced to a scalar equation, which is comparatively easy to solve.

4 Examples

4.1 Rolling Stone

This example tracks a point moving friction-less on a convex surface representing an idealized rolling stone. It can be considered as a harmonic oscillator provided the surface is parabolic. We modify this parabola by inserting a planar section in the interval $[-1, 1]$. This yields

$$V(z) = ((1+z)^2/2)\chi_{(-\infty, -1]}(z) + ((1-z)^2/2)\chi_{[1, \infty)}(z) \quad (10)$$

with χ denoting the characteristic function of the indexed set. The derivative of V defining the acceleration \ddot{z} of the mass is piecewise linear and given by

$$-V'(z) = \min(\max(-1-z, 0), 1-z) = -z - |z-1|/2 + |z+1|/2 \quad (11)$$

which yields the ODE $\ddot{z} = -V'(z)$. The analytic solution of the problem is $2\pi + 4$ periodic and given by

$$x(t) = \begin{cases} 1 + \sin(t) & 0 \leq t \leq \pi \\ 1 - (t - \pi) & \pi \leq t < \pi + 2 \\ -1 - \sin(2 - t) & \pi + 2 \leq t < 2\pi + 2 \\ t - 3 - 2\pi & 2\pi + 2 \leq t < 2\pi + 4 \end{cases}$$

In Figure 2 we depicted V and V' as well as the analytic solution of the ODE. The linear parts are drawn in gray.

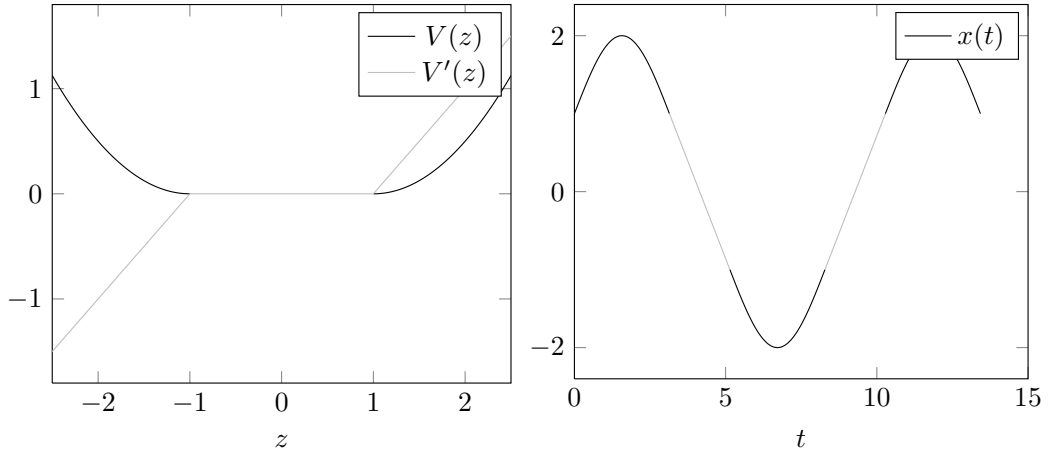


Figure 2: Visualization of V and the analytic solution of the ODE

From the second order ODE we obtain the first order system

$$\begin{pmatrix} \dot{x}_1 \\ \dot{x}_2 \end{pmatrix} = \begin{pmatrix} x_2 \\ -x_1 - |x_1 - 1|/2 + |x_1 + 1|/2 \end{pmatrix} = \begin{pmatrix} f_1(x_1, x_2) \\ f_2(x_1, x_2) \end{pmatrix} = F(x) \quad (12)$$

and observe, that the piecewise linearization by tangents, $\Delta F(\hat{x}, (\hat{x} - \check{x}) \cdot)$, equals the one based on secants, $\Delta F(\hat{x}, \check{x}; (\hat{x} - \check{x}) \cdot)$ since F is piecewise linear itself. We will consider the initial conditions $x_1(0) = 1$ and $x_2(0) = 1$ and the time interval $[0, 40]$. Given a step size h and applying the usual implicit midpoint rule to (12) yields the equations

$$\begin{aligned} \hat{x}_1 - \check{x}_1 &= hf_1\left(\frac{\hat{x}_1 + \check{x}_1}{2}, \frac{\hat{x}_2 + \check{x}_2}{2}\right) = h\left(\frac{\hat{x}_2 + \check{x}_2}{2}\right) \\ \hat{x}_2 - \check{x}_2 &= hf_2\left(\frac{\hat{x}_1 + \check{x}_1}{2}, \frac{\hat{x}_2 + \check{x}_2}{2}\right) = h\left[-\frac{\hat{x}_1 + \check{x}_1}{2} - 0.5\left|\frac{\hat{x}_1 + \check{x}_1}{2} - 1\right| + 0.5\left|\frac{\hat{x}_1 + \check{x}_1}{2} + 1\right|\right] \end{aligned}$$

where \tilde{x}_1, \tilde{x}_2 represent the current point and \hat{x}_1, \hat{x}_2 need to be computed. Substituting the second line into the first we obtain the piecewise linear equation

$$\hat{x}_1 = \tilde{x}_1 + \frac{h}{2} \left[2\tilde{x}_2 + h \left(-\frac{\hat{x}_1 + \tilde{x}_1}{2} - 0.5 \left| \frac{\hat{x}_1 + \tilde{x}_1}{2} - 1 \right| + 0.5 \left| \frac{\hat{x}_1 + \tilde{x}_1}{2} + 1 \right| \right) \right]. \quad (13)$$

The nonlinear RHS is contractive for sufficiently small step sizes h which then ensures the existence of \hat{x}_1 . Analogously, we can construct the scalar equation

$$\hat{x}_1 = \tilde{x}_1 + \frac{h}{2} \left[2\tilde{x}_2 + h \left(-\frac{\tilde{x}_1 + \hat{x}_1}{2} - \frac{|\tilde{x}_1 - 1| + |\hat{x}_1 - 1|}{4} + \frac{|\tilde{x}_1 + 1| + |\hat{x}_1 + 1|}{4} \right) \right] \quad (14)$$

from the classical trapezoidal rule. Again the existence of a solution follows from the Banach fix point theorem for sufficiently small h . Finally we consider the generalized midpoint rule for the ODE system (12).

$$\hat{x}_1 - \tilde{x}_1 = h \int_{-\frac{1}{2}}^{\frac{1}{2}} f_1(\hat{x}_1 + \tau(\hat{x}_1 - \tilde{x}_1), \hat{x}_2 + \tau(\hat{x}_2 - \tilde{x}_2)) d\tau = h \frac{\tilde{x}_2 - \hat{x}_2}{2} \quad (15)$$

$$\hat{x}_2 - \tilde{x}_2 = h \int_{-\frac{1}{2}}^{\frac{1}{2}} f_2(\hat{x}_1 + \tau(\hat{x}_1 - \tilde{x}_1), \hat{x}_2 + \tau(\hat{x}_2 - \tilde{x}_2)) d\tau = h \left(-\frac{\tilde{x}_1 + \hat{x}_1}{2} - \frac{\kappa_1}{2} + \frac{\kappa_2}{2} \right) \quad (16)$$

with

$$\kappa_1 = \int_{-\frac{1}{2}}^{\frac{1}{2}} \underbrace{\left| \frac{\hat{x}_1 + \tilde{x}_1}{2} - 1 + \tau(\hat{x}_1 - \tilde{x}_1) \right|}_{=: \frac{1}{2} \alpha_1} d\tau \quad \text{and} \quad \kappa_2 = \int_{-\frac{1}{2}}^{\frac{1}{2}} \underbrace{\left| \frac{\hat{x}_1 - \tilde{x}_1}{2} - 1 + \tau(\hat{x}_1 - \tilde{x}_1) \right|}_{=: \frac{1}{2} \alpha_2} d\tau.$$

Both terms can be computed and yield

$$\int_{-\frac{1}{2}}^{\frac{1}{2}} |\alpha_i + \tau\beta| = \begin{cases} \frac{1}{2} |\alpha_i| & \text{if } |\beta| < |\alpha_i| \\ \frac{\alpha_i^2 + \beta^2}{4|\beta|} & \text{else} \end{cases}$$

for $i = 1, 2$. Substituting (15) into (16) yields the nonlinear scalar equation

$$\hat{x}_1 = \tilde{x}_1 + h\tilde{x}_2 - \frac{h^2}{4} (\tilde{f}_1 + \tilde{x}_1 + \hat{x}_1 - \tilde{f}_2) \quad (17)$$

where \hat{x}_1 has to be computed.

If we approximate the solution of the ODE with (17) on the given time interval $[0, 40]$ for time steps $h > 0$ we observe the predicted global convergence order (proposition 3.1 and 3.2) of $O(h^2)$. The classical methods (trapezoidal rule based on (14) and implicit midpoint rule based on (13)) also yield a global convergence order $O(h^2)$ as shown in Figure 3 (a). Here we display the discretization error in the position coordinate x_1 . The error in the velocity coordinate x_2 is of similar magnitude. This behavior results from the fact, that nondifferentiabilities in the right hand side of (13) only occur 4 times per full period $2\pi + 4$ of the system and thus the local truncation error of the classical methods is only reduced in very few subintervals of $[0, 40]$. Moreover, this number stays constant for any time step size below a certain bound. Nevertheless we can observe that the generalized methods do not only converge with second order as predicted, but they are more stable than the classical methods, so we actually have an improvement. In fact there is even a more visible improvement, if we look at the energy of the whole system. As a frictionless mechanic system, the energy must be completely conserved by the analytic solution [2]. Hence $V(x(t)) + 1/2\dot{x}(t)^2$ must stay constant at its initial value $1/2$. Thus we consider the summed energy variation over the complete time interval using the formula

$$\left[\sum_{l=1}^{T/h} (V(x_1^l) + 1/2(x_2^l)^2 - 1)^2 \right]^{1/2}.$$

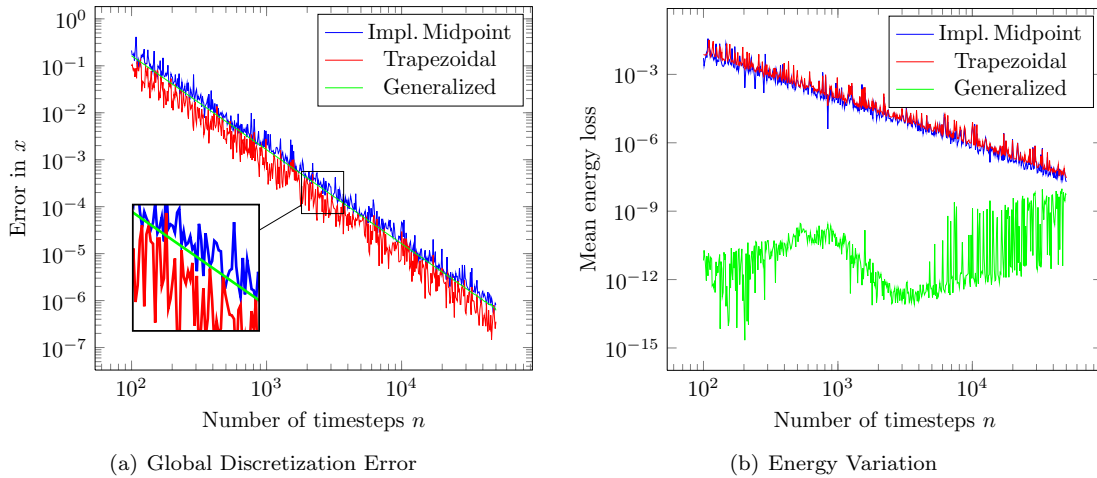


Figure 3: Results of Rolling Stone Example

The result is depicted in Figure 3 (b). As we see, the energy error is shrinking with smaller timestep h for the classical methods, but for the generalized method it is close to zero even for big timesteps. It increases for smaller timesteps due to rounding errors, but nevertheless the generalized methods are much closer to the desired behavior here.

4.2 Diode

As a second example we want to consider one similar to those arising in practical application. For that we take a simple LC-circuit and replace the resistor with a diode providing an element which causes a nondifferentiable impact in the equations describing the system. Figure 4 depicts the circuit. It is modeled by the following system of ODE's, where x_1 represents time, x_2 represents

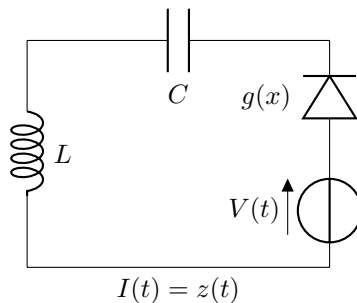


Figure 4: Circuit Diagram

the charge (at the capacitor) and x_3 represents the electric current in the circuit.

$$\begin{pmatrix} \dot{x}_1 \\ \dot{x}_2 \\ \dot{x}_3 \end{pmatrix} = F(\mathbf{x}) = \begin{pmatrix} 1 \\ x_3 \\ -(x_2 - CV(x_1) + g(Cx_3))\frac{1}{LC} \end{pmatrix} \quad (18)$$

Here $V(x_1) = \sin(\omega x_1)$ is the forcing current and $g(z)$ models the diode (for small currents) in the piecewise linear form

$$g(z) = \frac{z + |z|}{2\alpha} + \frac{z - |z|}{2\beta} = \begin{cases} \frac{z}{\alpha} & \text{if } z \geq 0 \\ \frac{z}{\beta} & \text{if } z < 0. \end{cases}$$

We choose the following values for the constants. They are similar to those in actual electric circuits.

$$L = 10^{-6}, C = 10^{-13}, \omega = 3 \cdot 10^9, \alpha = 2, \beta = 0.00001$$

Moreover, we consider the initial conditions $x_1(0) = x_2(0) = x_3(0) = 0$. Using the same techniques as in the last example, we can derive the classical and generalized midpoint and trapezoidal rules and transform them analogously into nonlinear scalar equations in \hat{x}_3 .

For the classical implicit midpoint rule we get the three equations:

$$\begin{aligned}\hat{x}_1 - \check{x}_1 &= h \implies \hat{x}_1 = \check{x}_1 + h \\ \hat{x}_2 - \check{x}_2 &= h \frac{\hat{x}_3 + \check{x}_3}{2} \implies \hat{x}_2 = \check{x}_2 + h \frac{\hat{x}_3 + \check{x}_3}{2} \\ \hat{x}_3 - \check{x}_3 &= -\frac{h}{LC} \left[\frac{\hat{x}_2 + \check{x}_2}{2} - C \sin \left(\omega \frac{\hat{x}_1 + \check{x}_1}{2} \right) + C \left(\frac{\dot{\hat{x}}_3 + |\dot{\hat{x}}_3|}{2\alpha} + \frac{\dot{\hat{x}}_3 - |\dot{\hat{x}}_3|}{2\beta} \right) \right].\end{aligned}$$

Substituting the first two into the third, we arrive at the scalar equation

$$\hat{x}_3 = \check{x}_3 - \frac{h}{LC} \left[\left(\check{x}_2 + \frac{h\hat{x}_3}{2} \right) - C \sin \left(\omega \frac{2\hat{x}_1 + h}{2} \right) + C \left(\frac{\dot{\hat{x}}_3 + |\dot{\hat{x}}_3|}{2\alpha} + \frac{\dot{\hat{x}}_3 - |\dot{\hat{x}}_3|}{2\beta} \right) \right]. \quad (19)$$

which is piecewise linear. For the classical trapezoidal rule we get

$$\begin{aligned}\hat{x}_1 - \check{x}_1 &= h \implies \hat{x}_1 = \check{x}_1 + h \\ \hat{x}_2 - \check{x}_2 &= h \frac{\hat{x}_3 + \check{x}_3}{2} \implies \hat{x}_2 = \check{x}_2 + h \frac{\hat{x}_3 + \check{x}_3}{2} \\ \hat{x}_3 - \check{x}_3 &= -\frac{h}{LC} \left[\frac{\hat{x}_2 + \check{x}_2}{2} - C \frac{(\sin(\omega\hat{x}_1) + \sin(\omega\check{x}_1))}{2} \right. \\ &\quad \left. + \frac{C}{2} \left(\frac{\hat{x}_3 + |\hat{x}_3|}{2\alpha} + \frac{\hat{x}_3 - |\hat{x}_3|}{2\beta} + \frac{\check{x}_3 + |\check{x}_3|}{2\alpha} + \frac{\check{x}_3 - |\check{x}_3|}{2\beta} \right) \right],\end{aligned}$$

which yields

$$\begin{aligned}\hat{x}_3 = \check{x}_3 - \frac{h}{LC} \left[\left(\check{x}_2 + \frac{h\hat{x}_3}{2} \right) - C \frac{(\sin(\omega(\check{x}_1 + h)) + \sin(\omega\check{x}_1))}{2} + \right. \\ \left. + \frac{C}{4} \left(\frac{1}{\alpha} + \frac{1}{\beta} \right) (\hat{x}_3 + \check{x}_3) + \frac{C}{4} \left(\frac{1}{\alpha} - \frac{1}{\beta} \right) (|\hat{x}_3| + |\check{x}_3|) \right].\end{aligned} \quad (20)$$

For the generalized midpoint rule we have:

$$\begin{aligned}\hat{x}_1 - \check{x}_1 &= h \implies \hat{x}_1 = \check{x}_1 + h \\ \hat{x}_2 - \check{x}_2 &= h \frac{\hat{x}_3 + \check{x}_3}{2} \implies \hat{x}_2 = \check{x}_2 + h \frac{\hat{x}_3 + \check{x}_3}{2} \\ \hat{x}_3 - \check{x}_3 &= -\frac{h(\check{x}_2 + \hat{x}_2)}{2LC} - \frac{h}{LC} \int_{-\frac{1}{2}}^{\frac{1}{2}} \left[-C \sin \left(\omega \frac{\hat{x}_1 + \check{x}_1}{2} \right) + \right. \\ &\quad \left. + C \left(\frac{\dot{\hat{x}}_3 + |\dot{\hat{x}}_3 + \tau(\hat{x}_3 - \check{x}_3)|}{2\alpha} + \frac{\dot{\hat{x}}_3 - |\dot{\hat{x}}_3 + \tau(\hat{x}_3 - \check{x}_3)|}{2\beta} \right) \right] d\tau \\ &= -\frac{h(\check{x}_2 + \hat{x}_2)}{2LC} + \frac{h}{L} \sin \left(\omega \frac{\hat{x}_1 + \check{x}_1}{2} \right) - \\ &\quad - \frac{h\dot{\hat{x}}_3}{2L} \left(\frac{1}{\alpha} + \frac{1}{\beta} \right) - \frac{h}{2L} \left(\frac{1}{\alpha} - \frac{1}{\beta} \right) \int_{-\frac{1}{2}}^{\frac{1}{2}} |\dot{\hat{x}}_3 + \tau(\hat{x}_3 - \check{x}_3)| d\tau.\end{aligned}$$

Substitution yields:

$$\hat{x}_3 = \check{x}_3 - \frac{h(2\check{x}_2 + h\dot{\check{x}}_3)}{2LC} + \frac{h}{L} \sin\left(\omega \frac{2\check{x}_1 + h}{2}\right) - \frac{h\dot{\check{x}}_3}{2L} \left(\frac{1}{\alpha} + \frac{1}{\beta}\right) - \frac{h}{2L} \left(\frac{1}{\alpha} - \frac{1}{\beta}\right) \varphi(\hat{x}_3), \quad (21)$$

with

$$\varphi(\hat{x}_3) = \begin{cases} \frac{1}{2} |\hat{x}_3 + \check{x}_3| & \text{if } |\hat{x}_3 - \check{x}_3| < |\hat{x}_3 + \check{x}_3| \\ \frac{(\hat{x}_3 + \check{x}_3)^2 + (\hat{x}_3 - \check{x}_3)^2}{4|\hat{x}_3 - \check{x}_3|} & \text{else} \end{cases}.$$

Finally for the generalized trapezoidal rule we get the following:

$$\begin{aligned} \hat{x}_1 - \check{x}_1 = h &\implies \hat{x}_1 = \check{x}_1 + h \\ \hat{x}_2 - \check{x}_2 = h \frac{\hat{x}_3 + \check{x}_3}{2} &\implies \hat{x}_2 = \check{x}_2 + h \frac{\hat{x}_3 + \check{x}_3}{2} \\ \hat{x}_3 - \check{x}_3 = -\frac{h(\check{x}_2 + \hat{x}_2)}{2LC} - \frac{h}{LC} \int_{-\frac{1}{2}}^{\frac{1}{2}} &\left[-C \frac{(\sin(\omega \hat{x}_1) + \sin(\omega \check{x}_1))}{2} + \right. \\ &\left. + C \left(\frac{|\hat{x}_3 + |\dot{\hat{x}}_3 + \tau(\hat{x}_3 - \check{x}_3)||}{2\alpha} + \frac{|\check{x}_3 - |\dot{\check{x}}_3 + \tau(\hat{x}_3 - \check{x}_3)||}{2\beta} \right) \right] d\tau \\ &= -\frac{h(\check{x}_2 + \hat{x}_2)}{2LC} + \frac{h}{L} \frac{(\sin(\omega \hat{x}_1) + \sin(\omega \check{x}_1))}{2} - \\ &\quad - \frac{h\dot{\check{x}}_3}{2L} \left(\frac{1}{\alpha} + \frac{1}{\beta}\right) - \frac{h}{2L} \left(\frac{1}{\alpha} - \frac{1}{\beta}\right) \int_{-\frac{1}{2}}^{\frac{1}{2}} |\hat{x}_3 + \tau(\hat{x}_3 - \check{x}_3)| d\tau. \end{aligned}$$

Again, substituting the first two equations into the third, we arrive at:

$$\hat{x}_3 = \check{x}_3 - \frac{h(2\check{x}_2 + h\dot{\check{x}}_3)}{2LC} + \frac{h}{L} \frac{(\sin(\omega(\check{x}_1 + h)) + \sin(\omega \check{x}_1))}{2} - \frac{h\dot{\check{x}}_3}{2L} \left(\frac{1}{\alpha} + \frac{1}{\beta}\right) - \frac{h}{2L} \left(\frac{1}{\alpha} - \frac{1}{\beta}\right) \varphi(\hat{x}_3), \quad (22)$$

where $\varphi(\hat{x}_3)$ is defined as above. This yields a piecewise linear scalar equation in one variable, which we can solve with standard methods.

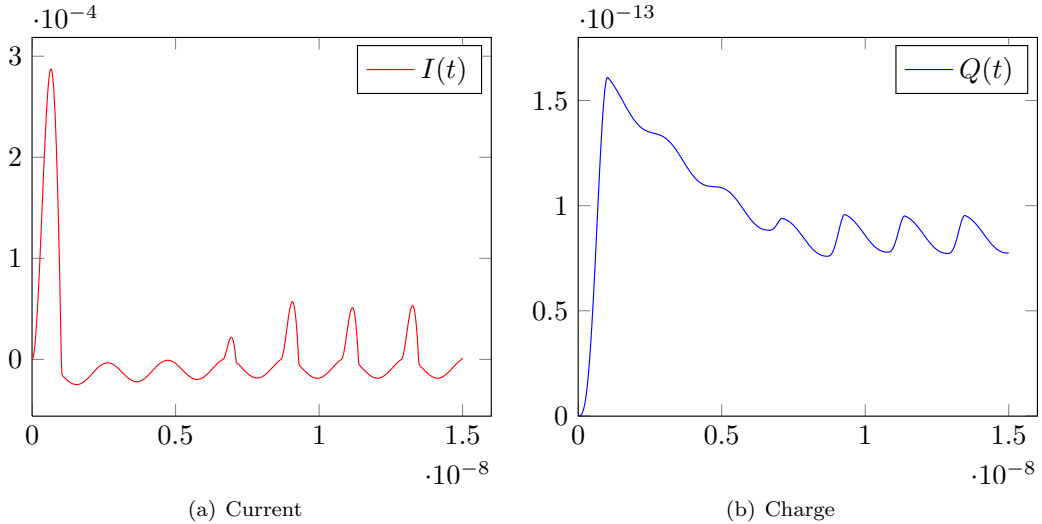


Figure 5: Solution of the ODE System

The result of the numerical integration solution of (18) is depicted in Figure 5, (a) and (b). As one can see, the capacitor is initially charged over one cycle and discharged over a few more, before

the solution adopts a periodic behavior. The solution trajectory changes its behavior every time the current changes its sign. As in the first example, the new and the old methods show second order convergence. Here we have plotted the relative error in the coordinate x_1 representing the current. For the classical methods based on (19) and (20) this follows from the fact that there are only finitely many kinks along the trajectory. However, the generalized methods based on (22) and (21) are more stable as depicted in Figure 6, where we can see the relative error of the current.

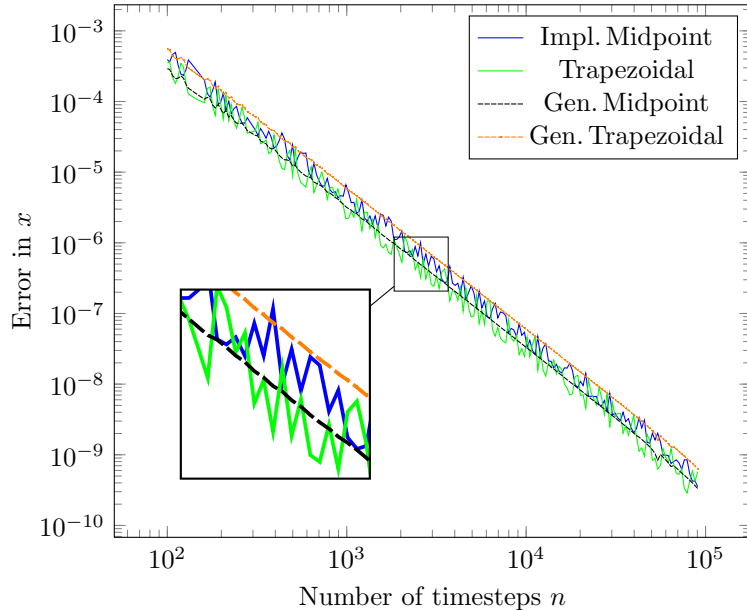


Figure 6: Global Discretization Error

5 Conclusions and Outlook

In this paper we studied the validity of theoretical results from [3, 7] concerning the integration of ODE's with Lipschitz continuous but nondifferentiable right hand sides, on two examples. As required by the theory, the nondifferentiabilities exhibit a certain structure, namely they are defined in terms of the absolute value function. We have observed that, as predicted the global order of convergence for the numerical approximations of the solutions to the ODE's is indeed 2. This was achieved by the so called generalized trapezoidal and generalized midpoint rule introduced in [3]. A detailed derivation of the particular discretized equations for the two example problems is provided. The equations are a little more complicated but reduce to the classical discretization over all time steps where the right hand side does not cross a kink. Where they do, the defining equations of the classical rules are also only semi-smooth so that the numerical solution requires some care. We expect that with a good implementation the new schemes will not require significantly more runtime than the old ones.

Naturally, we compared the convergence accuracy of the generalized methods to the classical trapezoidal and implicit midpoint rule. Besides the stabilizing effect of the new approach we observed a much better energy preservation of the generalized integration method on the simple Hamiltonian systems represented by Example 1. Now the fluctuation in the total energy error stays, in contrast to the classical methods at the working accuracy level, until too many small steps accumulate too much round off. Unfortunately, it seems clear that on nonsmooth Hamiltonian systems neither the original nor the generalized midpoint rule are symplectic. I

It is hoped that for Lipschitzian Hamiltonian systems of the kind consider here the fluctuation of the energy due to the new discretizations can be bounded theoretically, naturally disregarding round-off as customary. The natural continuation of this work is the application to examples, where the influence of the occurring absolute values clearly degrades the convergence order of the classical integration methods. Moreover, setting up and solving the piecewise linear equations (17), (21) and (22) is certainly laborious and error prone. A method to obtain these solutions based on [3] automatically is currently under development. It uses the AD package ADOL-C [5] and a numerical linear algebra package PLAN-C to construct and solve these equations in the so called abs-normal form by various Newton like methods and fix point solvers. For detailed information we refer to [6] and [1].

Finally we wish to enhance the methods presented here by providing a cubic $C^{1,1}$ interpolant of the solution trajectory. Finally, we wish to develop an error estimator and on that basis a step size control. As of now, it seems unlikely that a higher than second order variant of the methods proposed here can be developed.

References

- [1] Boeck, P. *Implementation and Application of the Generalized Midpoint Rule for Lipschitzian ODE's*, Diploma Thesis, HU Berlin, 2014
- [2] Chartier, P. and Faou, E. *Geometric integrators for piecewise smooth Hamiltonian systems*, M2AN, vol. 48(2), 2008, pp 223 - 241
- [3] Griewank, A. *On stable piecewise linearization and generalized algorithmic differentiation*, OMS, vol. 28(6), 2013
- [4] Griewank, A. and Walther, A. *Evaluating derivatives: principles and techniques of algorithmic differentiation*, SIAM, 2008
- [5] Griewank, A. and Juedes, D. and Mitev, H. and Utke, J. and Vogel, O. and Walther, A. *ADOL-C: A Package for the Automatic Differentiation of Algorithms Written in C/C++*, ACM TOMS, vol. 22(2) June 1996, pp. 131-167, Algor. 755
- [6] Griewank, A. and Bernt, J.-U. and Radons, M. and Streubel, T. Solving piecewise lineare equations in abs-normal form. Submitted to *Linear Algebra and its Application*.
- [7] Hasenfelder, R. *Numerische Validierung verallgemeinerter Mittelpunkts- und Trapezregeln zur Integration von Lipschitz-stetigen DGL's*, Bachelors Thesis, HU Berlin, 2013
- [8] Naumann, U. *The Art of Differentiating Computer Programs*, SIAM, 2012
- [9] Scholtes, S. *Introduction to piecewise differentiable equations*, Springer, 2012